INSTITUTE OF PHYSICS PUBLISHING JOURNAL OF PHYSICS D: APPLIED PHYSICS

J. Phys. D: Appl. Phys. **37** (2004) 2810–2813 PII: S0022-3727(04)80717-4

Tin oxide transparent thin-film transistors

R E Presley[1], C L Munsee[1], C-H Park[2], D Hong[1], J F Wager[1] and D A Keszler[2]

[1] School of Electrical Engineering and Computer Science, 220 Owen Hall, Oregon State University, Corvallis, OR 97331-3211, USA
[2] Department of Chemistry, 153 Gilbert Hall, Oregon State University, Corvallis, OR 97331-4003, USA

E-mail: jfw@ece.orst.edu

Received 14 May 2004, in final form 30 July 2004
Published 29 September 2004
Online at stacks.iop.org/JPhysD/37/2810
doi:10.1088/0022-3727/37/20/006

Abstract

A SnO_2 transparent thin-film transistor (TTFT) is demonstrated. The SnO_2 channel layer is deposited by RF magnetron sputtering and then rapid thermal annealed in O_2 at 600°C. The TTFT is highly transparent, and enhancement-mode behaviour is achieved by employing a very thin channel layer (10–20 nm). Maximum field-effect mobilities of 0.8 $cm^2\,V^{-1}\,s^{-1}$ and 2.0 $cm^2\,V^{-1}\,s^{-1}$ are obtained for enhancement- and depletion-mode devices, respectively. The transparent nature and the large drain current on-to-off ratio of 10^5 associated with the enhancement-mode behaviour of these devices may prove useful for novel gas-sensor applications.

The majority of transparent thin-film transistors (TTFTs) reported to date have employed ZnO as a channel material (Carcia *et al* 2003, Hoffman *et al* 2003, Masuda *et al* 2003, Nishi *et al* 2003, Norris *et al* 2003, Wager 2003, Hoffman 2004). A notable exception is the high-performance $InGaO_3(ZnO)_5$ superlattice TTFT whose single-crystal channel layer can be considered to be composed of alternating layers of InO_2^- and $GaO(ZnO)_5^+$ (Nomura *et al* 2003). The purpose of the work reported herein is to demonstrate a new type of TTFT in which the channel layer is SnO_2.

SnO_2 thin-film transistors (TFTs) have been reported previously (Klasens and Koelmans 1964, Aoki and Sasakura 1970, Prins *et al* 1996, 1997, Wöllenstein *et al* 2003). All these SnO_2 TFTs are depletion-mode devices, requiring the application of a gate voltage to turn them off. Prins *et al* (1996) fabricated a SnO_2 : Sb TFT on a transparent $SrTiO_3$ substrate with a $PbZr_{0.2}Ti_{0.8}O_3$ ferroelectric gate insulator and an opaque $SrRuO_3$ gate. The SnO_2 TFT reported by Wöllenstein *et al* (2003) is noteworthy since the utility of such a device as a novel gas sensor is demonstrated. In contrast to what has been reported previously, the SnO_2 TFT reported herein operates as an enhancement-mode device, requiring the application of a gate voltage to turn the device on. Although several strategies were investigated to achieve enhancement-mode operation, as discussed below, our only successful approach was to decrease the channel thickness to approximately 10–20 nm in order to minimize current flow through the 'bulk' portion of the channel layer. We believe that the large drain current on-to-off ratio of 10^5, associated with enhancement-mode operation, and the optical transparency of the SnO_2 TTFTs discussed herein offer further advantages for novel gas-sensor applications.

Bottom-gate SnO_2 TTFTs are fabricated on glass substrates, manufactured by the Nippon Sheet Glass Company, coated with 200 nm sputtered indium tin oxide (ITO) and a 220 nm atomic layer deposited superlattice of Al_2O_3 and TiO_2 (ATO)[3]. The ITO and ATO layers constitute the gate contact and insulator, respectively. Typically, the channel layer is deposited by RF magnetron sputtering using a tin oxide target (Cerac) in Ar/O_2 (97%/3%) at a pressure of 5 m Torr, power density of ∼3 W cm^{-2}, target-to-substrate distance of ∼7.5 cm, and no intentional substrate heating. The channel layers are typically 10–20 nm thick. The channel length and width are 1524 μm and 7620 μm, respectively. Alternatively, SnO_2 channel layers are formed either by thermal evaporation at a pressure of $\sim 10^{-6}$ Torr or by activated reactive evaporation in either microwave-activated O_2 or N_2 at a pressure of $\sim 5 \times 10^{-4}$ Torr. In both cases, SnO_2 powder is used as the evaporation source material. After deposition of the SnO_2 channel layer the sample is annealed, typically via furnace or rapid thermal annealing (RTA) in O_2 at 600°C. Finally, ITO source and drain contacts are formed by ion-beam sputtering.

Figure 1 displays the dc drain-current–drain-voltage (I_{DS}–V_{DS}) characteristics for a SnO_2 TTFT. The slopes of most

[3] ITO/ATO glass was supplied by Arto Pakkala, Planar Systems, Inc. Espoo, Finland, arto_ pakkala@planar.com.

of the I_{DS} curves shown in figure 1 are extremely flat at large V_{DS}, indicating that a condition of 'hard saturation' is achieved, due to complete pinch-off of the channel. However, the two uppermost I_{DS} curves exhibit a small slope since the condition for pinch-off, i.e. $V_{DS} \geqslant V_{GS} - V_T$ (where V_T is the threshold voltage), is not achieved. It is evident from figure 1 that the TTFT is essentially off, at least with respect to the 90 μA scale used for this figure. This implies enhancement-mode behaviour (i.e. negligible current flows at zero gate voltage; a positive gate voltage is required to turn on the drain current).

A positive threshold voltage, $V_T \simeq 10$ V, is obtained from extrapolation of the linear portion of the dc drain-current–gate-voltage (I_{DS}–V_{GS}) characteristic, as shown in the insert in figure 2, indicating this to be an enhancement-mode device. However, as evident from the log(I_{DS})–V_{GS} transfer characteristics shown in figure 2, the turn-on voltage, corresponding to the gate voltage at which the channel current first begins to increase (Hoffman 2004), is approximately −20 V. Thus, a very large negative voltage is required to completely turn off the device. Note also from figure 2 that the gate leakage current for this device is very small, less than 1 nA, and that the drain current on-to-off ratio is quite large, $\sim 10^5$. It is apparent from figure 2 that this device has a poor inverse subthreshold slope of approximately 4 V decade^{-1}.

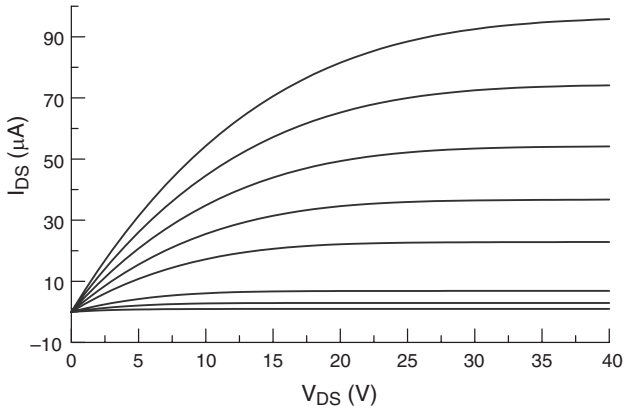

Figure 1. I_{DS}–V_{DS} characteristics for a SnO_2 TTFT with a SnO_2 channel layer that is ∼10 nm thick, deposited by RF magnetron sputtering, and rapid thermal annealed in O_2 at 600°C. The channel length and width are 1524 μm and 7620 μm, respectively. V_{GS} is decreased from 40 (top curve, showing maximum current) to 0 V in 5 V steps.

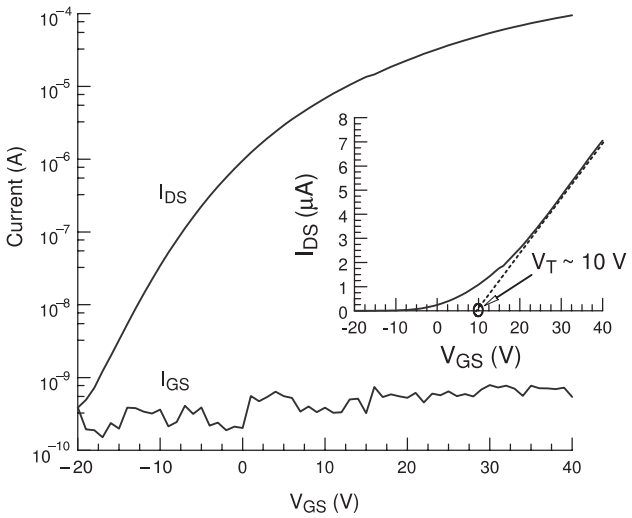

Figure 2. Log(I_{DS})–V_{GS} and log(I_{GS})–V_{GS} characteristics at $V_{DS} = 35$ V for a SnO_2 TTFT with a channel width-to-length ratio of 5. Inset shows an extrapolation of the linear portion of an I_{DS}–V_{GS} curve, resulting in an estimated threshold voltage of $V_T \simeq 10$ V. The SnO_2 channel layer is ∼10 nm thick, deposited by RF magnetron sputtering, and rapid thermal annealed in O_2 at 600°C.

Although the threshold voltage assessed from figure 1 and from the insert in figure 2 both indicate the SnO_2 TTFT to be enhancement-mode, it is clearly evident from figure 2 that a very large negative voltage is required to completely turn the device off. The essential attribute of enhancement-mode operation of significance is the drastic increase in the drain current on-to-off ratio with enhancement-mode operation. Note from figure 2 that a threshold voltage of −20 to −25 V, typical of what we observe for our depletion-mode TTFTs, would have a drain current on-to-off ratio less than 10. Thus, from an application point of view, our achievement of enhancement-mode operation has significantly improved the drain current dynamic range, which may prove advantageous if this device is employed as a gas sensor.

As seen from the I_{DS}–V_{DS} curves shown in figure 1, the TTFT exhibits a maximum drain current near 90 μA, a modest value for a TTFT with a channel width-to-length ratio of 5. The magnitude of I_{DS} depends on the mobility of the electrons in the channel. The maximum field-effect mobility (Schroder 1998) for the enhancement-mode device corresponding to figure 1 is equal to 0.8 cm^2 V^{-1} s^{-1}. The maximum field-effect mobility is 2 cm^2 V^{-1} s^{-1} for our depletion-mode SnO_2 TTFTs.

The optical transmittance versus wavelength through the ITO source/drain and channel of a SnO_2 TTFT is shown in figure 3. Curve (a) is the transmittance corrected for reflectance, i.e. $T/(1-R)$, indicating an average transmission of ∼90% across the visible spectrum (400–700 nm). Curve (b) is the raw transmittance through the entire stack, including the substrate, indicating an average transmission of ∼75% across the visible spectrum.

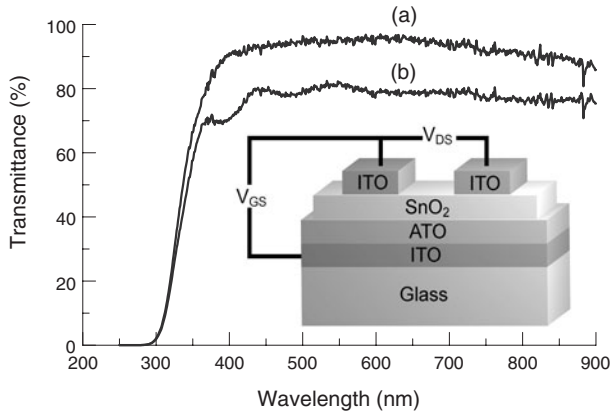

Figure 3. Optical transmittance as viewed through the ITO source/drain and the channel of a SnO_2 TTFT. Curve (a) is corrected for reflectance, i.e. $T/(1-R)$, whereas curve (b) is the raw transmission through the entire stack, including the substrate. Inset illustrates the bottom-gate TTFT structure and biasing scheme employed.

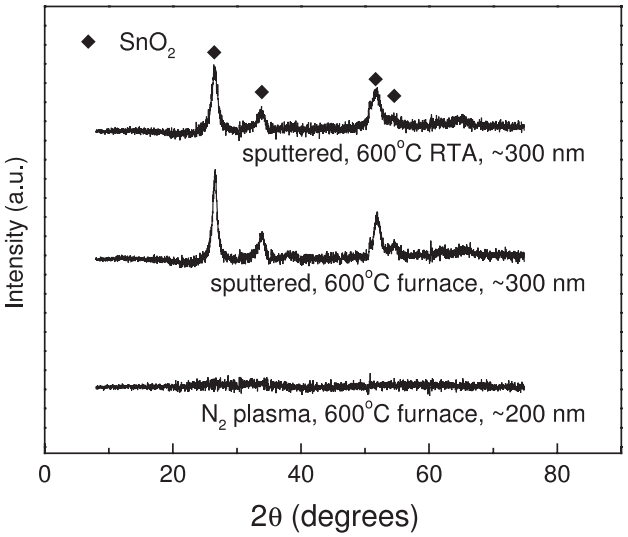

Figure 4. XRD patterns obtained from two sputter-deposited SnO_2 thin films which are either furnace or rapid thermal annealed at 600°C, and for a SnO_2 thin film prepared by evaporation of SnO_2 powder in a $\sim 5 \times 10^{-4}$ Torr pressure of microwave-activated N_2 and subsequently furnace annealed at 600°C. The post-deposition anneal leads to increased crystallinity of the sputtered films, whereas films prepared by activated reactive evaporation in N_2 remain amorphous after annealing.

We have found it very difficult to fabricate enhancement-mode SnO_2 TTFTs. Although our 'as deposited' SnO_2 thin films are invariably extremely insulating, they exhibit little or no gate modulation when employed as TTFT channel layers due to poor crystallinity, thus requiring a post-deposition anneal.

Figure 4 shows an x-ray diffraction (XRD; performed with a Siemens D-5000 x-ray diffractometer using Cu Kα radiation) comparison of two sputter-deposited SnO_2 thin films, which are heated at 600°C with a furnace or RTA. Peak identification confirms these films to be SnO_2. Assessment of the XRD peak widths, using the Scherrer formula and a Lorentzian peak shape, yields an estimated average crystal size of 11 nm (furnace) and 7.5 nm (RTA), whereas Williamson–Hall plots give average crystal size, strain estimates of 17.1 nm, 0.023% (furnace) and 16.5 nm, 0.036% (RTA) (Cullity and Stock 2001). The Williamson–Hall analysis suggests that the RTA film is more strained than the furnace annealed film, and that the Scherrer formula significantly underestimates the crystal size due to the neglect of strain.

Improving the crystallinity of the SnO_2 thin film via a post-deposition anneal does not ensure enhancement-mode TTFT behaviour. Typically, our annealed SnO_2 thin films are too conductive for TTFT applications, presumably due to the tendency of SnO_2 to form oxygen vacancies, which are shallow double-donors providing conduction-band electrons (Samson and Fonstad 1973, Hartnagel *et al* 1995). Often the channel-layer conductivity is so high that it cannot be appreciably modulated by a gate voltage, making transistor operation impossible. If the channel-layer conductivity is sufficiently lowered, transistor behaviour is possible, although such TFTs operate in depletion mode unless the conductivity can be decreased to an appropriate level.

We have explored several methods for reducing the conductivity of the SnO_2 channel layer. One approach is to evaporate SnO_2 powder in a partial pressure of microwave-activated N_2. The idea here is to incorporate nitrogen into the SnO_2 film, since nitrogen substitution onto an oxygen atomic site results in acceptor doping which would compensate oxygen vacancies or other SnO_2 donors, thereby reducing both the carrier concentration and the conductivity of the film. Although films prepared in this manner are indeed highly resistive, they unfortunately remain amorphous after heat treatment at 600°C. Thus, TTFTs fabricated with such films as channel layers do not exhibit transistor action, presumably due to the very poor mobility of these amorphous films. Figure 4 includes the XRD pattern of such a film, confirming its amorphous nature. We also explored compensation of SnO_2 films by indium diffusion doping, since indium substitution onto a tin atomic site also results in acceptor doping. Although indium incorporation into the SnO_2 film did result in a decrease in conductivity, as expected, we could never achieve the required degree of conductivity control of the channel with this doping. To date, our most successful approach for minimizing the channel-layer conductivity is to increase the resistance of a relatively conductive SnO_2 channel by simply decreasing the channel thickness; this is our motivation for employing very thin channel layers ($\sim$10–20 nm).

In conclusion, we have fabricated a highly transparent SnO_2 TTFT with prototypical I_{DS}–V_{DS} characteristics, a modest channel mobility, and enhancement-mode behaviour. The enhancement-mode nature of these SnO_2 TTFTs results in an I_{DS} on-to-off ratio of $\sim 10^5$, which is approximately four orders of magnitude larger than that of a depletion-mode device. This improvement in the I_{DS} on-to-off ratio should dramatically increase the dynamic range of SnO_2 TFT gas sensors as proposed by Wöllenstein *et al* (2003). Moreover, the transparent nature of SnO_2 TTFTs may lead to improved sensor performance and new sensor applications, since heterogeneous processes occurring at the active sensor surface may be optically stimulated or probed from the sensor side opposite gas/analyte exposure.

Acknowledgments

This work was funded by the US National Science Foundation under Grant No DMR-0071727 and by the Army Research Office under Contract No MURI E-18-667-G3.

References

Aoki A and Sasakura H 1970 *Japan. J. Appl. Phys.* **9** 582
Carcia P F, McLean R S, Reily M H and Nunes G 2003 *Appl. Phys. Lett.* **82** 1117–19
Cullity B D and Stock S R 2001 *Elements of X-Ray Diffraction* 3rd edn (Upper Saddle River, NJ: Prentice-Hall)
Hartnagel H L, Dawar A L, Jain A K and Jagadish C 1995 *Semiconducting Transparent Thin Films* (Bristol: Institute of Physics)
Hoffman R L, Norris B J and Wager J F 2003 *Appl. Phys. Lett.* **82** 733–5
Hoffman R L 2004 *J. Appl. Phys.* **95** 5813–19
Klasens H A and Koelmans H 1964 *Solid-State Electron.* **7** 701–2
Masuda S, Kitamura K, Okumura Y, Miyatake S, Tabata H and Kawai T 2003 *J. Appl. Phys.* **93** 1624–30

Nishi J *et al* 2003 *Japan. J. Appl. Phys.* **42** L347–9
Nomura K, Ohta H, Ueda K, Kamiya T, Hirano M and Hosono H 2003 *Science* **300** 1269–72
Norris B J, Anderson J, Wager J F and Keszler D A 2003 *J. Phys. D: Appl. Phys.* **36** L105–7
Prins M W J, Grosse-Holz K-O, Müller G, Cillessen J F M, Giesbers J B, Weening R P and Wolf R M 1996 *Appl. Phys. Lett.* **68** 3650–2
Prins M W J, Zinnemers S E, Cillessen J F M and Giesbers J B 1997 *Appl. Phys. Lett.* **70** 458–60
Samson S and Fonstad C G 1973 *J. Appl. Phys.* **44** 4618–21
Schroder D K 1998 *Semiconductor Material and Device Characterization* 2nd edn (New York: Wiley)
Wager J F 2003 *Science* **300** 1245–6
Wöllenstein J, Jägle M and Böttner H 2003 *Advanced Gas Sensing* ed T Doll (Boston: Kluwer Academic) pp 85–99